Investigation of Rectifier Diode Failures in the NEXT-C Power Processing Unit

George L. Thomas,* Henry B. Fain,* David C. Pike*, Luis R. Piñero†,
Marcelo C. González*, Robert J. Scheidegger‡,
NASA Glenn Research Center, Cleveland, Ohio, 44135

Scott R. Panko§, and Arthur G. Birchenough**
HX5, Cleveland, Ohio, 44135

NASA's Evolutionary Xenon Thruster-Commercial (NEXT-C) project is tasked with developing flight electric propulsion systems, including both thrusters and power processing units (PPUs). In 2018, the beam supply in a NEXT-C engineering prototype PPU experienced an output rectifier diode failure during development thermal-vacuum testing. A failure investigation led by NASA GRC identified the root cause of the failure as a thermal runaway caused by increased reverse recovery losses in the diodes when the PPU was run at its maximum operating temperature. Significant reverse recovery performance variations were identified in diodes with the same part number but manufactured by different vendors. The failure investigation was able to collect evidence of the increased reverse recovery and replicate the diode failures in a controlled laboratory environment.

I. Introduction

The NASA Evolutionary Xenon Thruster Commercial (NEXT-C) project had the goal to develop flight thrusters and PPUs for use on future NASA missions sponsored by the Planetary Science Division, within the Science Mission Directorate (SMD) [1-3]. The precursor to this project known as NASA Evolutionary Xenon Thruster (NEXT), initially started under the NASA In-Space Propulsion Technology Program developing key components for a 7 kW gridded ion propulsion system at the NASA Glenn Research Center (GRC). This development effort included the design and fabrication of a high-fidelity brassboard PPU [4-8]. NEXT-C was a follow-on project that advanced the propulsion system development by designing, fabricating, and testing a prototype PPU [9-10]. Subsequently, the first NEXT-C flight string was delivered to Johns Hopkins University Applied Physics Laboratory (APL) for use on the Double Asteroid Redirection Test (DART) Mission scheduled to launch in 2021.

During development of the prototype PPU, several issues were encountered with the output diodes for the beam supply, including sourcing them from the heritage vendor, part-to-part and vendor-to-vendor variations in diode performance that contributed to part failures at nominal conditions, and even failures due to operation in inadvertent off-nominal conditions. A failure investigation was led by GRC to identify the root-cause of the latest part failure and assess the implications to future applications of NEXT-C. This paper summarizes the finding and conclusions of the failure investigation.

II. NEXT-C PPU Design

The NEXT-C PPU was designed to throttle the thruster from 0.5 to 6.9 kW of power while operating from an input voltage of 80 to 160 V. It contains four power supplies that process power for the thruster. The beam supply processes most of that power, up to 6.34 kW at an output voltage range from 275 to 1800 volts. The beam supply consists of six modules that operate in parallel to supply the required beam current. These modules are individually

* Electrical Engineer, Power Management and Distribution Branch
† Senior Electrical Engineer, Electric Propulsion Systems Branch
‡ Supervisory Electrical Engineer, Power Management and Distribution Branch
§ Electrical Engineer, Materials and Structures Division
** Electrical Engineer, Power Management and Distribution Branch

addressable such that loading can be optimized for any particular thruster throttling condition. The beam modules use an innovative dual-bridge topology and a six-diode rectifier, shown in Figure 1.

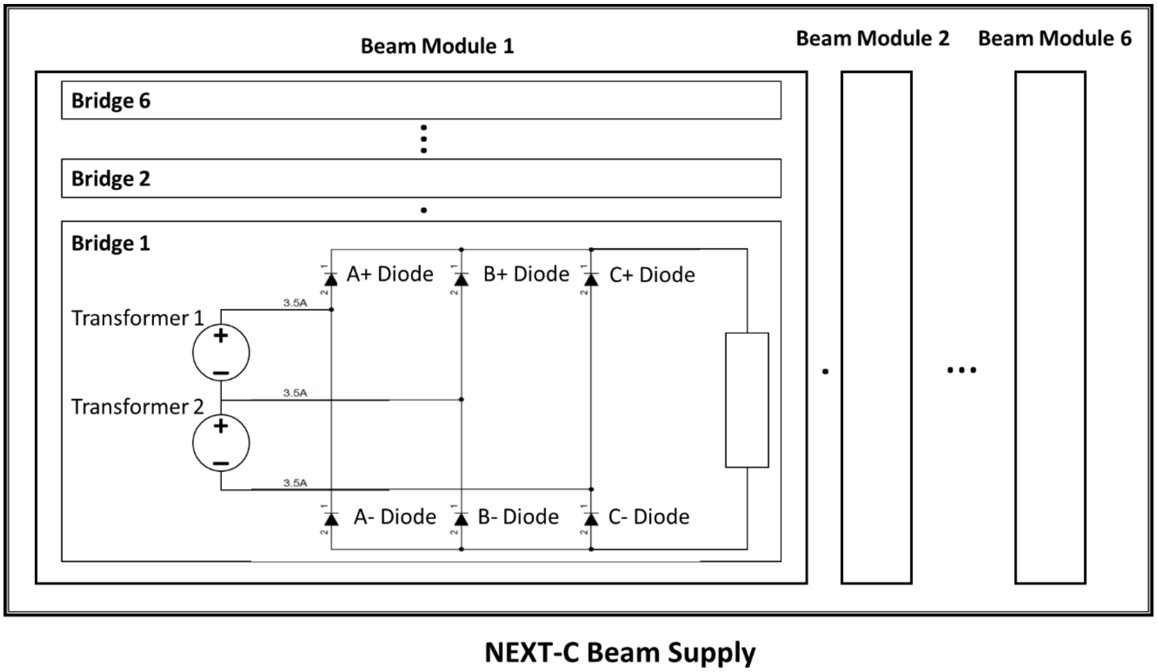

Figure 1. Diagram of NEXT-C beam supply, showing its modular construction.

Each beam module has six rectifiers, each generating up to 300 V and stacked in series to generate up to 1800 V. Two modes of operation, pulse-width modulation (PWM) and phase-shift modulation (PSM) enable the wide range of operation with high efficiency. PWM mode operates the transformer secondary windings for the dual-bridge converters in parallel such that the average output voltage increases with duty-cycle. Once the duty-cycle maximizes, the beam module enters PSM mode in which the dual bridge converters overlap their operation such that the transformer secondary windings operate in series which effectively doubles the transformer turns ratio and a 2x boost in output voltage. This converter demonstrated efficiencies well in excess of 95 percent. Figure 2 shows a brassboard beam module, built by the contractor of the precursor NEXT project. The input assembly, on the left, includes the inverter and control printed circuit boards (PCB) and the output assembly, on the right, includes the power transformers for the dual-bridge converters and three output PCBs for the six output rectifier stages.

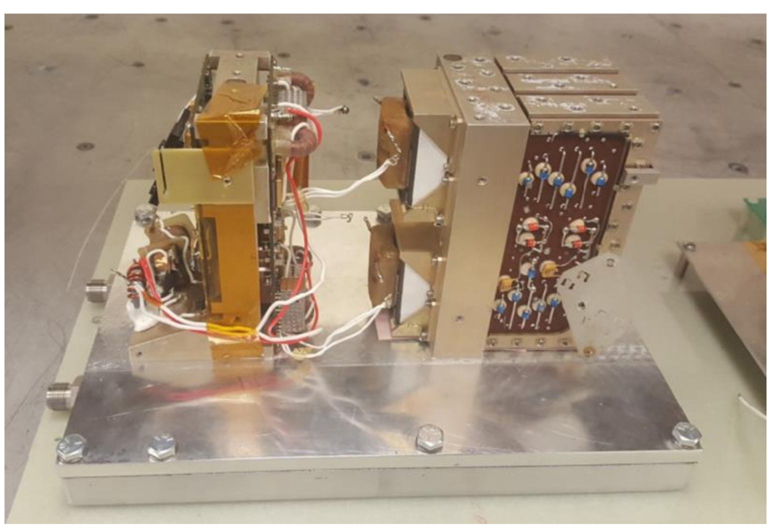

Figure 2. Single beam module with controller and rectifier assemblies

III. Failure Conditions

The baseline NEXT brassboard PPU used through-hole 1N6631 diodes from a qualified part list (QPL) vendor. Note that the 1N6631 datasheet specifies a reverse voltage of 1 kV and a maximum forward current of 1.8 A (assuming a lead temperature of 75 ºC). We will refer to the part used for NEXT as Diode Xa. The NEXT-C PPU was designed by the PPU contractor to use surface-mount 1N6631 diodes. The contractor had difficulty sourcing Diode Xa parts because the vendor was relocating their manufacturing facility. While they were able to acquire a partial quantity from old stock of Diode Xa, they also sourced 1N6631 diodes from another QPL vendor which we will refer to as Diode Y. The NEXT-C prototype PPU was built using both diodes, where entire beam modules were populated with one of these two diodes.

During a thermal-vacuum (TVAC) test of the prototype PPU, several diodes from a beam module populated with Diode Y failed. A failure investigation conducted by the contractor concluded that the Diode Y parts were most likely operating at higher temperatures than Diode Xa parts due to higher reverse recovery losses. An evaluation of reverse recovery losses of all previous diodes and some new candidates was conducted at precisely controlled operating conditions and temperature to identify the best candidates for this design. The vendor of Diode Xa was contacted during the investigation and informed that Diode Xa was being manufactured under a new process in their new factory and provided samples of their new part. Note that the heritage part is referred to as Diode Xa to contrast it with the new part produced by the same vendor, which we call Diode Xb. Also included in the study was Diode Y and a new candidate Diode Z. The measurements revealed that the best diode in terms of reverse recovery performance was Diode Xa, which was the original part, followed by Diode Z and Diode Xb with fairly close results. The worst performer was Diode Y that had previously experienced failures. Since Diode Xa is discontinued and Diode Xb was not yet in production, Diode Z was selected for this design. The prototype PPU was rebuilt with one of the six beam modules (beam module #6) populated with commercial Diode Z parts, and the remaining beam modules populated with available stock of heritage Diode Xa. At the same time, a lot of flight diodes was ordered for flight model PPUs. Note that flight diodes are subjected to a custom screening process for a variety of performance criteria, including reverse recovery performance.

Subsequently, during a second TVAC test of the prototype PPU, the beam supply was inadvertently operated at a loading condition higher than intended but well within its voltage and current rating during the seventh of ten consecutive temperature cycles. The beam supply was meant to operate with four modules, 1396 V, and 2.3 A or 0.58 A per module. Instead, it was operated at 2.7 A or 0.68 A per module. After approximately an hour of operation at a baseplate temperature of 55˚C, beam module #6 failed. The remaining TVAC test plan was completed using the remaining five beam modules.

The failure was attributed to the incorrect operating condition and the prototype PPU was rebuilt using spare flight components (Diode Z) to continue PPU development testing. However, some concerns remained among the NEXT-C team about the ability of these diodes to operate at NEXT-C full power conditions and the amount of operational margin on diode current since the overload only constituted a 17 percent increase in diode current. Further, the 0.68 A per module current seen by the diodes is less than half of the nominal 1N6631 maximum current rating of 1.8 A, indicating that the diode should have been well within its current capabilities. These concerns prompted the NASA-led failure investigation that is the subject of this paper.

IV. Failure Investigation

A. Hypotheses

Several possibilities were suggested to explain these failures, including imbalance between the series output rectifier modules in the circuit, imbalance between transformer output channels feeding the rectifiers, insufficient peak suppression in the rectifier snubber circuit (voltage stress), thermal runaway due to problems in the thermal design or otherwise, and parts issues. Although the failure occurred during a slight overload test condition, the diodes were still operated well within their voltage and current derated levels, assuming the circuit was balanced per the design.

Imbalance was suggested as a possibility, because imbalance could cause one or more diodes to see a peak voltage or current above the part rating. Voltage stress was also proposed, as the snubber circuit was designed with minimal capacitance, to avoid damping or slowing the diode voltages. This was done to keep switching losses low and achieve high efficiency. Thermal runaway and parts issues were also hypothesized, because previous iterations of the design had shown that some rectifier diode parts used in circuit were prone to thermal runaway from reverse recovery losses. A test plan was then designed to validate these hypotheses.

B. Destructive Part Analysis

Some of the failed and also pristine (brand new, untouched) Diode Z components were sent to the Goddard Space Flight Center (GSFC) Electrical Systems Failure Analysis Group for destructive part analysis (DPA). The results of the failed parts identified direct anode to cathode shorts, and junction damage due to molten silicon caused by electrical overstress. The pristine parts showed manufacturing defects including cracks in the anode and cathode dies and voids between the dies and the metal contacts as shown in Figure 3.

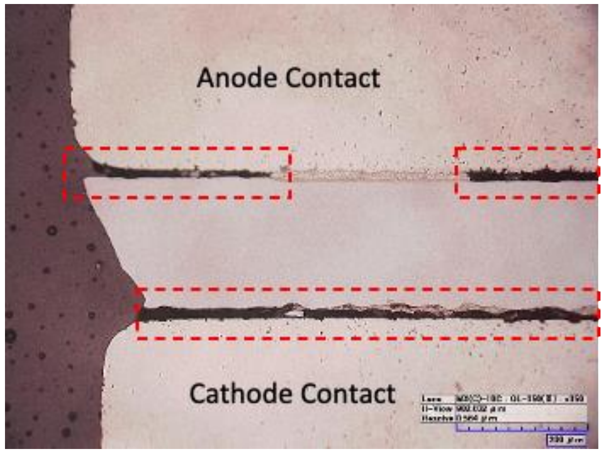

Figure 3. Photograph of cross section of virgin unscreened Diode Z showing voids between die and both anode and cathode contacts.

According to the manufacturer, these defects are common in commercial parts and can be responsible for the inferior performance and part-to-part variations. While these defects could have contributed to the failures experienced by the prototype PPU, they should not be a concern for flight part lots because they are typically detected by Group A part screening tests. Note that there was not sufficient time or resources to verify the manufacturer's claim that flight screening should eliminate these defects.

C. Testing Hardware and Instrumentation

Testing for the failure investigation was conducted on development hardware built during the precursor NEXT project. Shown in Figure 4 is the output assembly of a beam module breadboard. This assembly was originally populated with Diode Xa parts and allowed for easy part replacement to get baseline performance measurements. It was also used to collect data to assess the imbalance hypothesis as it provided easy access to all areas of the circuit.

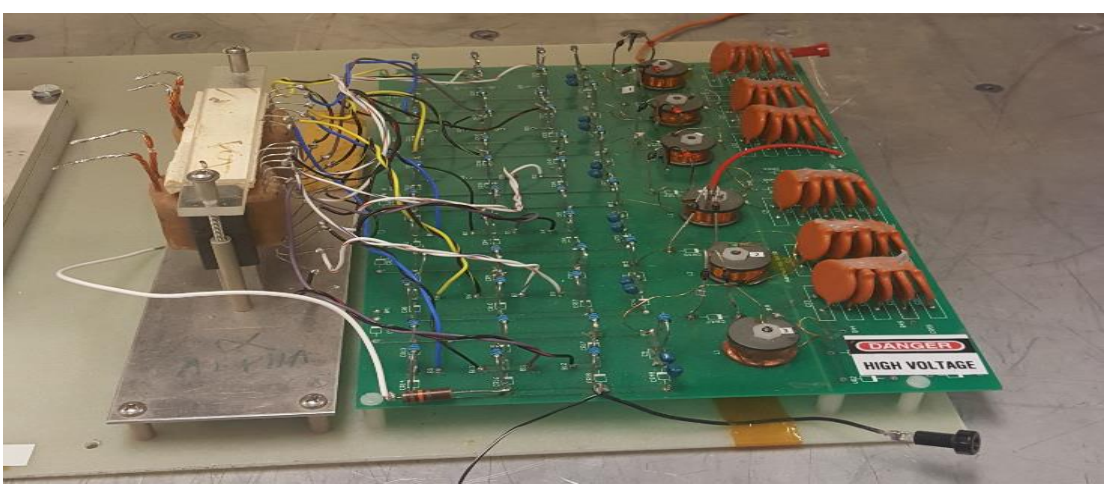

Figure 4. Breadboard beam module output assembly.

Shown in Figure 5 is the brassboard beam module also built during the NEXT project. It was designed for operation in vacuum and to dissipate all heat through a baseplate.

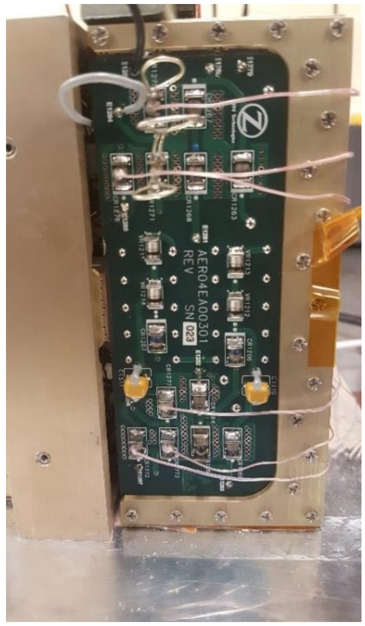

Figure 5. Brassboard beam module output assembly including prototype output PCB (populated with Diode Y parts) and thermocouples on lower bridge diodes

A heat exchanger was used to pump water through the baseplate (silver surface shown underneath the beam module in Figure 5) to control its temperature. The effects of convection cooling were reduced by covering the brassboard beam module with an insulated box when necessary for testing. The design of this module is the same as the NEXT-C prototype and flight PPUs. Although the original output PCBs in the brassboard beam module used Diode Xa parts, they were easily replaced with prototype PCBs that contained Diode Y and Diode Z parts when needed by the investigation to replicate the previous failures. However, only one of three output PCBs was replaced at any time. This was done to increase the chances of catching a diode failure in the prototype PCB populated with lower performance Diode Y and Z parts, as opposed to the higher performance Diode Xa parts in the original PCBs.

The brassboard beam module was operated at nominal and overload conditions similar to when the previous failures occurred with the goal of detecting an impending thermal runaway. Diode voltage and current measurements were collected via an oscilloscope in order to capture electrical signals indicating the cause of thermal runaway. High voltage differential probes were used to measure diode voltages using small and short sense leads soldered to the PCB pads. Diode currents were measured using isolated current probes attached to current sense loops. These loops were created by cutting PCB traces carrying the diode current and soldering a loop of wire to close the broken circuit. A wire gauge of 26 AWG was chosen for both voltage sense leads and current sense loops so they would have the smallest possible effect on the thermal performance of the instrumented diodes, noting that in earlier attempts heavier gauge wires were found to conduct heat away from the diodes and lower operating temperatures. Figure 6 shows the brassboard beam module with the differential voltage probes and a current probe connected to the circuit via the sense leads described above.

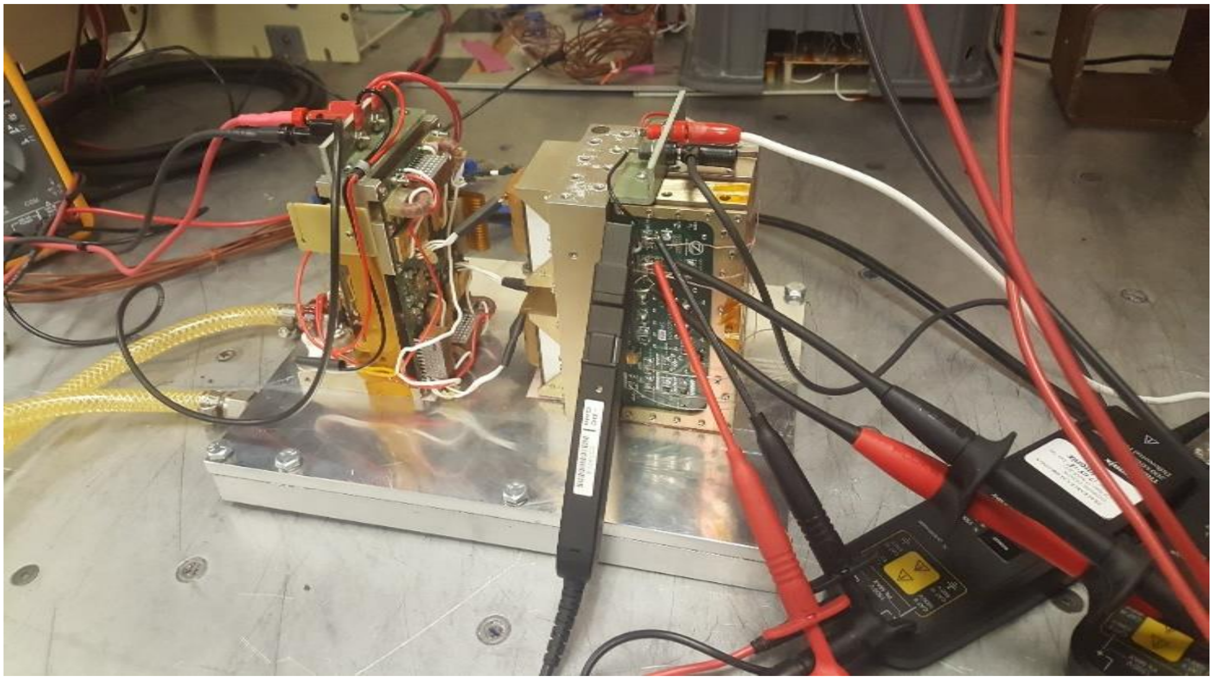

Figure 6. Brassboard beam module connected to test equipment.

These electrical measurements described above targeted diode B+ and B- in the lower rectifier bridge on the output PCB. The lower bridge has a lower floating voltage than the upper bridge because it is lower in the output stack of six rectifiers. The B+ and B- diodes see the full output current of the module when operating in the PWM mode, and so were expected to be the hottest and thus first to reach thermal runaway.

MATLAB scripts were written to collect and analyze oscilloscope voltage and current waveform data in real time. The scripts take the product of the voltage and current data for each diode instrumented, which yields an estimate of instantaneous diode power dissipation. The power dissipation is integrated when the diode is reverse conducting to obtain per-cycle reverse recovery energy estimates. The scripts were set up to calculate and display peak reverse current, peak reverse power and reverse recovery energy in real time during the tests. Finally, diode temperatures were measured with type-T thermocouples mounted onto the diode cases using two-part epoxy loaded with alumina powder to improve thermal conductivity while maintaining electrical isolation.

V. Breadboard Module Test Results

Initial testing during this effort was conducted using the breadboard beam module assemblies because its open construction provided easy access for simultaneous electrical measurements, including voltage and current on any diode or transformer secondary winding in any rectifier bridge. Multiple diode current measurements could be accessed while in operation. Testing focused on investigating a variety of possible failure modes including improper snubber circuit design and imbalance between the six stacked secondary windings.

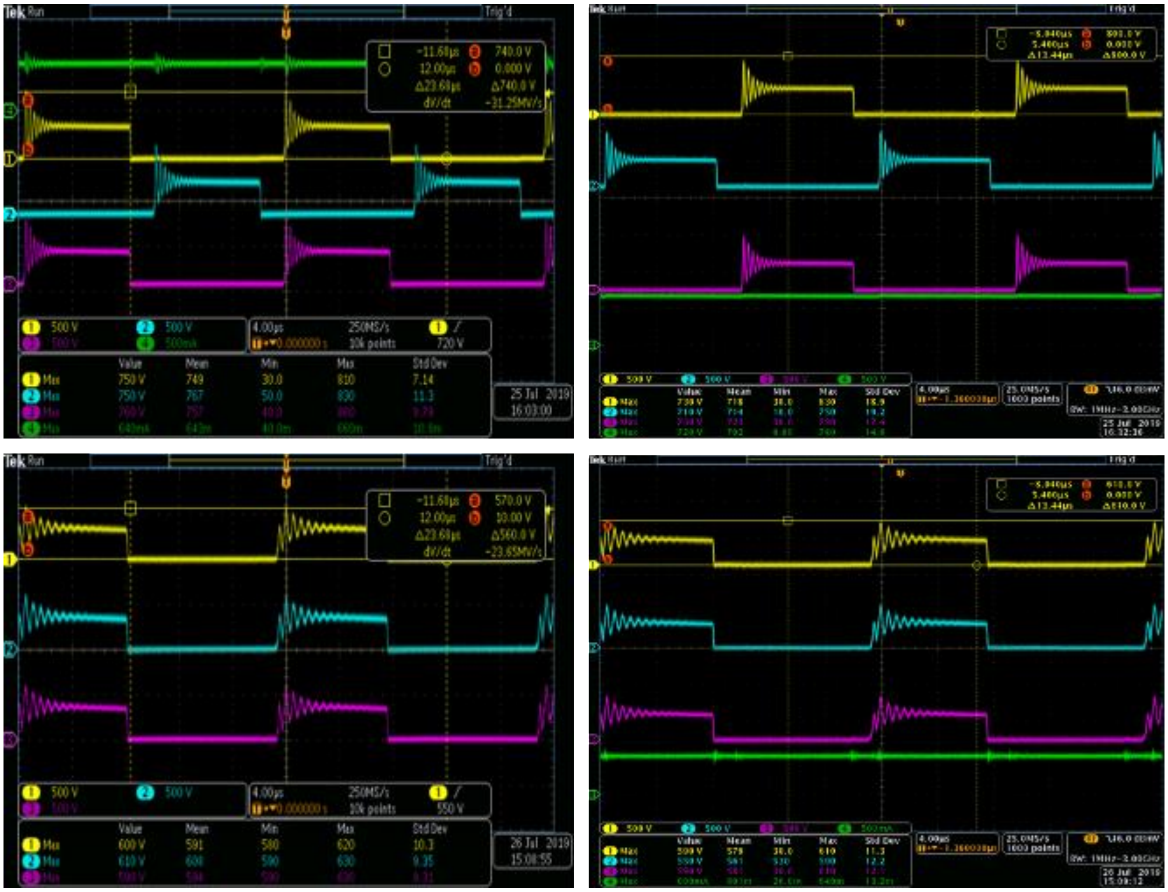

Figure 7. Diode voltages for all diodes within same bridge rectifier (top) and diode voltages on a diode for all six rectifier stages in the output series stack (bottom)

The top pictures in Figure 7 show in-circuit measurements on all six diodes (A+, B+, C+, A-, B- and C-) within the same output rectifier bridge. Besides the 180 degree phase shift expected during operation in PWM mode, the waveforms look symmetrical and without excessive resonances. The green trace on the top right is the voltage on the snubber capacitor that shows the expected DC voltage level without unexpected transients. The bottom pictures in Figure 7, show the voltage on diode A+ for each one of the six rectifier stages in the output series stack. As expected, all six waveforms are symmetrical, balanced and without excessive ringing. Only ambient temperature testing was completed with the breadboards because of difficulties in increasing and controlling its operating temperature. On the other hand, it is easy to control the operating temperature of the brassboard, because it is mounted to a baseplate and connected to a temperature controlled liquid heat exchanger. For that reason, testing transitioned to the brassboard model beam module.

VI. Brassboard Module Test Results

A. Diode Y Testing

The remaining tests were conducted on the brassboard beam module assembly. The module used was previously built during the NEXT project, and contained output PCBs populated with Diode Xa parts. One of the three output PCBs, each including two bridge rectifiers, were replaced with a prototype PCB assembled with unscreened, commercially available Diode Y parts. Since these parts had previously failed at ambient temperature conditions, it was expected that it would be easy to induce failure through testing. It was expected that the Diode Xa parts in the other two PCB would not fail due to their superior performance.

The objectives to these tests were, first, to characterize electrical and thermal performance of the diode at nominal load conditions (1800 V and 0.6 A) while operating at room and elevated temperatures. Second, to capture a thermal runaway condition on the diode by increasing the beam module baseplate temperature while operating at nominal and overload conditions (1800V and 0.75 A).

1. *Initial Diode Y Test*

For this test, all six diodes in the lower rectifier bridge were instrumented for thermal measurements. The initial test condition was an output voltage of 1800 V, output current of 0.6 A, and a baseplate temperature of 25 ˚C. The baseplate temperature was then raised. A failure occurred early in the testing at a baseplate temperature of 40 ºC. Diodes B+ and C+ on the upper bridge failed. Unfortunately, these upper bridge diodes were not instrumented at the time of failure and no data was captured.

This early failure was attributed to a weak or defective part since the Diode Y part were unscreened commercial parts. The test setup was then modified by replacing all the upper bridge Diode Y parts with Diode Z parts. This would increase the probability of a failure event to the lower bridge of the PCB since Diode Z parts were known from previous testing to be superior to Diode Y in terms of reverse recovery.

2. *Diode Y Baseline Test*

Testing was resumed after replacing the upper bridge diode parts. This test reached the previous 40 ºC baseplate temperature without failures so the baseplate temperature was increased further. It was found that no further runaway events could be induced while operating at the 1800 V, 0.6A test condition up to a baseplate temperature of 60 ºC. This test was considered a baseline, because it showed that the beam module could be run at elevated baseplate temperatures.

3. *Diode Y Runaway Test*

In an attempt to generate a runaway condition, the output current was increased from 0.60 A to 0.75 A while operating at 1800 V. This level is 25% higher than the NEXT-C maximum rated output current. The B+ and B- diodes on the lower bridge were observed to be the hottest diodes throughout the test. The B+ diode showed signs of the onset of thermal run away consistently at a baseplate temperature of 60 ºC. The beam module was turned off before a complete run away to prevent failure. This experiment was repeated three times with similar results. Temperature data of the runaway event is shown in Figure 8.

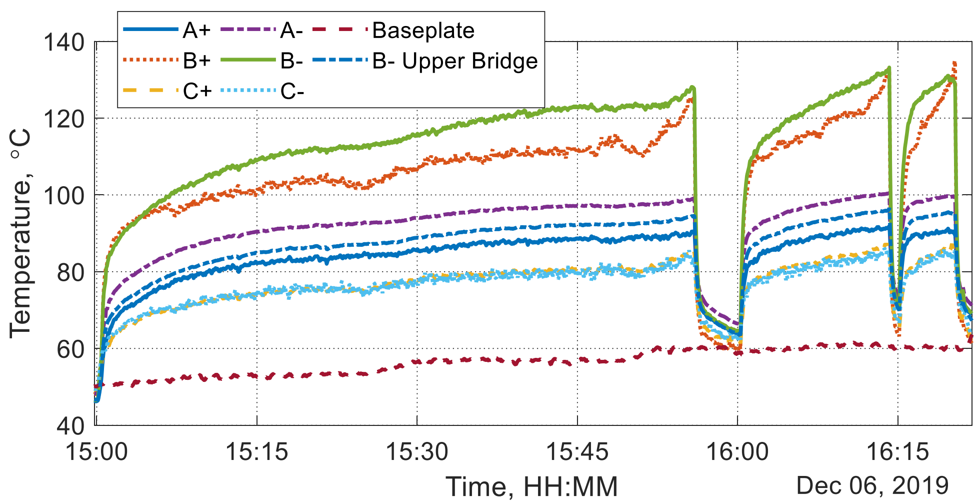

Figure 8. Graph of a thermal runaway event of Diode Y at a baseplate temperature of 60 ºC and output conditions of 1800 V, 0.75 A.

In-circuit reverse recovery measurements were conducted using the MATLAB scripts described in Section IV, subsection C. Figure 9 shows reverse recovery data computed by the scripts at two different B+ diode temperatures. Note that each unit energy shown on the plot represents 1/50 µJ. On the left, at 53 ˚C baseplate temperature, the B+ diode has a case temperature of 102 ˚C and a reverse recovery energy of approximately 36 µJ. On the right, a baseplate temperature of 59 ˚C, resulted in a diode case temperature of 132 ˚C and a reverse recovery energy of 60 µJ. The reverse recovery energy doubled with a small baseplate temperature increase of only 6 ˚C. Also, the diode conducts more current for a longer time during the reverse recovery event when it is hotter. This can be seen by comparing the magnitude of the reverse recovery current (especially the second spike), as well as the area under the power curve (the green areas in the figure).

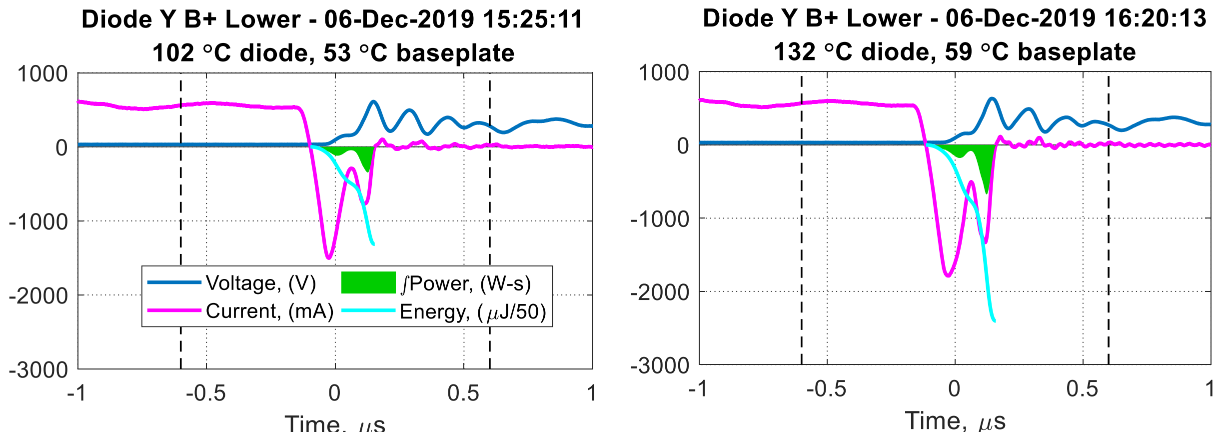

Figure 9. Reverse recovery waveforms for Diode Y, showing the B+ diode at a temperature of 102 ºC (left) and 132 ºC (right) at output conditions of 1800 V and 0.75 A.

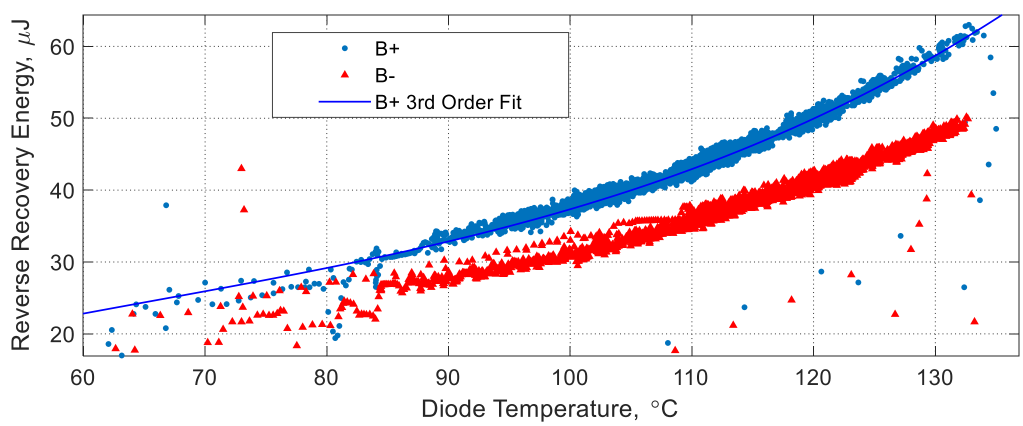

Figure 10. Diode temperature vs reverse recovery energy for the two hottest Diode Y parts during runaway test.

Figure 10 shows the relationship between reverse recovery energy and diode temperature. The data used to produce this figure are from the last power cycle of the test (the last 15 minutes of the test, as shown in Figure 8. This data shows that the B+ diode has greater reverse recovery losses than the B- diode at a given temperature. Also, the relationship between reverse recovery energy and diode temperature is nonlinear (and has an especially high slope for the B+ diode as it approaches runaway). Note that the absolute maximum operating junction temperature for the 1N6631 part is specified as 150 ºC. Given that the maximum glass diode body temperature measured during testing was 132 ºC, and that the junction temperature was likely significantly hotter due to the junction-to-body thermal resistance, it is likely that the junction temperature was near its limit. The trends in Figure 8 and Figure 10 suggest that the B+ diode would have likely gone into thermal runaway, exceeded its temperature limit, and failed if it was allowed to run for a slightly longer time. Another observation was that the temperature for the onset of thermal runaway was lower the more times the test was repeated. This suggest the diodes were being degraded by the operating conditions during the test.

B. Diode Z Testing

The Diode Y parts on the lower rectifier bridge used for the previous test were replaced with Diode Z parts. Since both upper and lower rectifier bridges in the PCB were then populated with Diode Z, we were unable to predict which rectifier bridge was likely to thermally runaway first. To avoid this, all 12 diodes were instrumented with thermocouples and in-circuit reverse recovery measurements were done on the B diodes of both upper and lower rectifier bridges.

1. Diode Z Baseline Test

The first test was a baseline test at nominal NEXT-C output conditions of 1800 V at 0.6 A. Figure 11 shows the temperature data taken during the test. At a baseplate temperature of 65 ºC, the hottest part was the B+ diode on the lower rectifier bridge, which had a case temperature of 95 ºC. This is significantly lower than the result with Diode Y, where at 60˚C baseplate some diodes were approaching 120 ˚C and showing signs of thermal runaway. The reduced temperature suggests that losses in the Diode Z parts are lower than in the Diode Y parts.

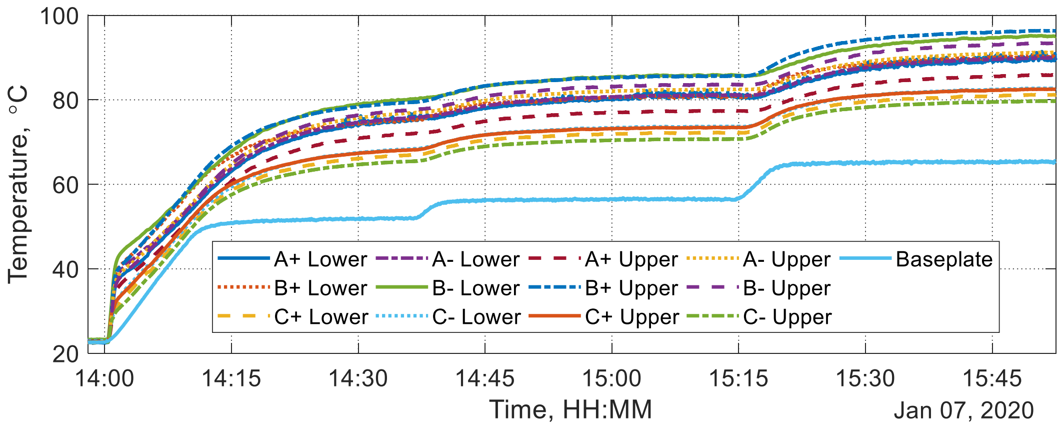

Figure 11. Baseline test on Diode Z at nominal NEXT-C output conditions of 1800 V and 0.6 A.

2. Diode Z Runaway Test

As before, the diodes current was increased from 0.6 to 0.75 A. Temperature data of the runaway event is shown in Figure 12 The B+ diode on the upper bridge showed signs of thermal run away at a baseplate temperature of 74 ºC. This result was consistent after three consecutive test cycles.

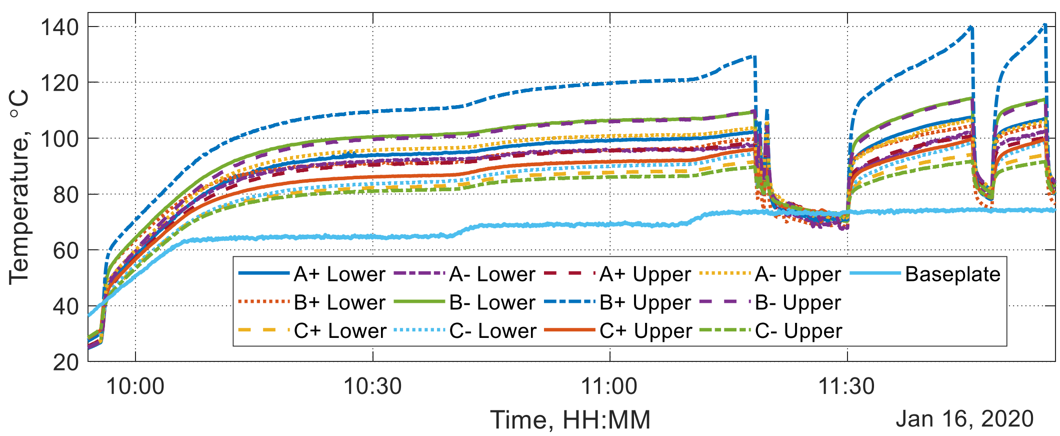

Figure 12. Runaway test on Diode Z at overload output conditions of 1800 V and 0.75 A.

Results of the in-circuit reverse recovery measurements from this test are shown in Figure 13. This data shows that Diode Z parts have approximately 22 µJ of reverse recovery energy and a case temperature of 110 ˚C at a baseplate temperature of 64 ˚C. This represents just 61% of the energy and 83% of the diode temperature measured on Diode Y parts at a slightly lower baseplate temperature of 59 ˚C. The reverse recovery performance of Diode Z is significantly better than Diode Y and required a higher baseplate temperature of 74 ˚C to onset thermal runaway. The reverse recovery energy at runaway was approximately 39 µJ, as shown on the right plot in Figure 13. Also, a case temperature of 139 ˚C was measured during runaway onset which is within 7˚C of the case temperature measured on Diode Y. Another interesting result is that while the current in Diode Z had higher peak values, the duration and average values were lower resulting in lower reverse recovery power and energy than Diode Y. One possible explanation is that Diode Z parts may switch faster than Diode Y parts under the conditions seen in this circuit.

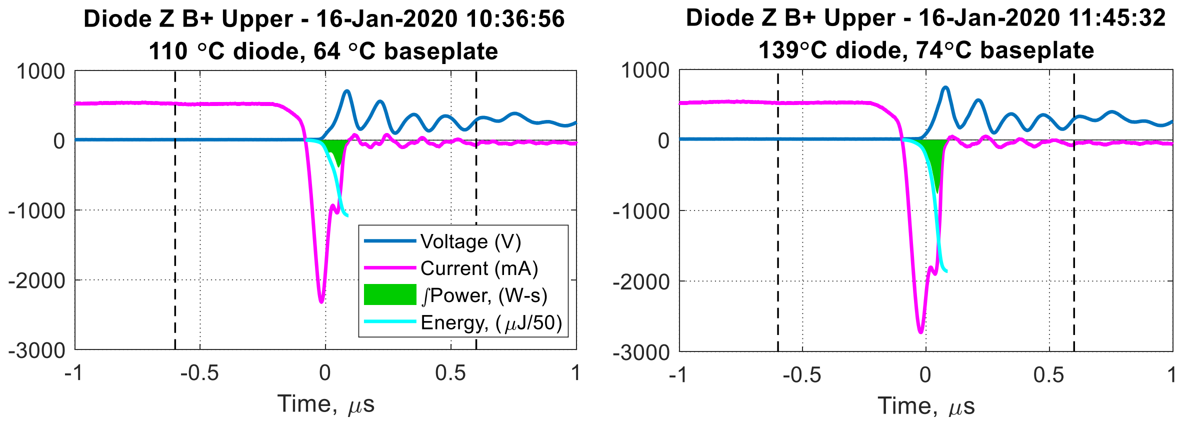

Figure 13. Reverse recovery waveforms for Diode Z, showing the B+ diode at a temperature of 110 ºC (left) and 139 ºC (right) at output conditions of 1800 V and 0.75 A.

The plot of reverse recovery loss versus diode temperature for the last power cycle is shown in Figure 14. The data shows the same non-linear behavior in the Diode Z part as seen in the Diode Y part, although with significantly less reverse recovery energy then Diode Y. Also, the increasing slope provides more evidence suggesting that the diode was approaching thermal runaway.

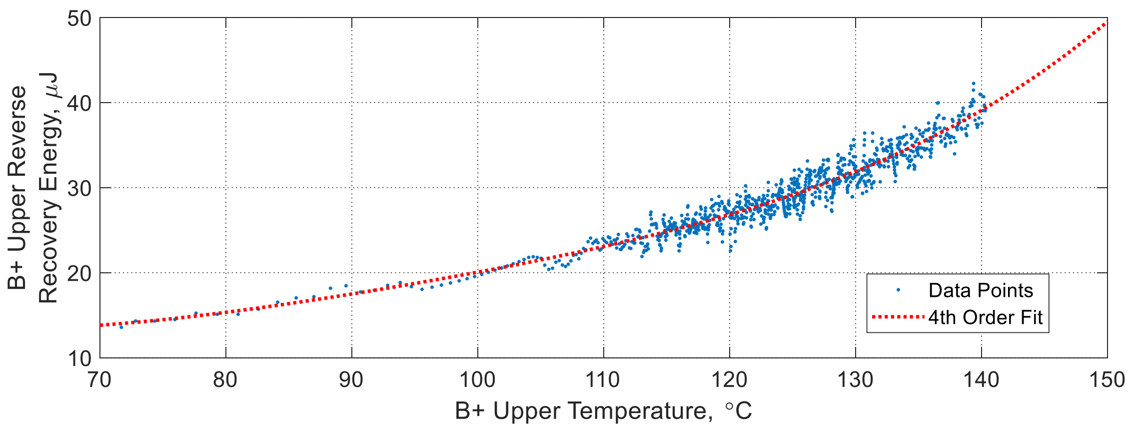

Figure 14. Diode temperature vs reverse recovery energy for the hottest Diode Z part (B+ upper bridge) during the Diode Z runaway test.

VII. Test Results Discussion

Comparing the test results between Diode Y and Diode Z allows drawing several conclusions about the root cause of the failures. While both diodes were able to operate at the NEXT-C maximum operating condition of 1800 V and 0.6 A, only a 25 % increase in output current to 0.75 A and just a fraction of its current rating, was able to push them into thermal runaway. Diode Z consistently operated at a lower average recovery current, power, and energy according to in-circuit measurements and lower case temperature. For this reason, it required higher baseplate temperatures than Diode Y to drive it into thermal runaway. Also, since the diode voltage during the turn-off cycles is fairly consistent, the average reverse recovery current drives the reverse recovery power and energy. Furthermore, the relationship between reverse recovery and temperature appeared to be nonlinear particularly when operating close to the runaway condition, with the increase in reverse recovery losses rising rapidly at higher temperatures. Additional analysis of the test results are shown in Figure 15 as plots of reverse recovery energy and temperature as a function of time. This data show that the slope of the reverse recovery energy starts to increase at a fast rate earlier than the temperature. This early "energy runaway" suggests that the increase in reverse recovery energy is the root cause of the problem while the higher operating case temperature is an effect that eventually leads the part to failure once the thermal runaway occurs.

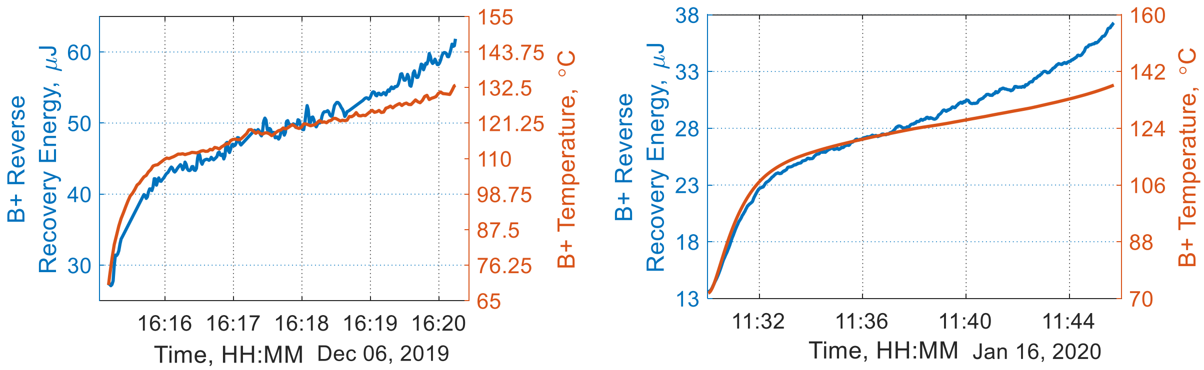

Figure 15: Reverse recovery energy and temperature as a function of time for Diode Y (left) and Diode Z (right)

Note, evidence of part-to-part variation was found during the course of testing. Some Diode Y parts were shown to fail at conditions within the NEXT-C operating limits, and other Diode Y parts on the same board, running in the same bridge location can be run beyond these limits (simultaneously 25% over max current and 5% above the maximum temperature during Diode Y runaway test). This data does not conclusively demonstrate margin, because the tests conducted in this investigation were all at ambient pressure and not the vacuum environment required for the NEXT-C PPU application. Additional vacuum chamber tests are planned to quantify this margin and conclusively show that the design is capable of full power in vacuum.

VIII. Conclusions

This paper presents testing efforts to determine the root cause of failure of diodes in the NEXT-C prototype PPU during thermal vacuum testing in 2018 to better understand how the part failed while it was operating within its current and temperature rating. Testing was conducted on parts with the same part number but manufactured by different vendors. DPA conducted at GSFC revealed that the commercial unscreened parts used for the prototype PPU and this investigation showed evidence of manufacturing defects that could have contributed to inferior performance and failures. Circuit measurements on a breadboard beam module verified that the operation of the innovative NEXT beam supply was balanced, symmetrical, and did not produce unexpected stresses on the diodes or any other component. Diode Y, which had failed in the prototype PPU, and Diode Z, which had been chosen as the replacement part, were tested during the investigation. Test data shows that Diode Y had higher operating temperature, average reverse current, and reverse recovery energy than Diode Z for a given baseplate temperature. Also, it was shown that Diode Y could be brought to the onset of thermal runaway at a lower baseplate temperature than Diode Z. In both diodes, the diode case temperature at which thermal runaway appeared to begin was approximately 135-140 ˚C. Further analysis of reverse recovery data showed the non-linear relationship between reverse recovery energy and diode temperature, and why it can lead the diode into a thermal runaway. The data also suggest that reverse recovery energy is the root cause of the failures since it starts increasing at an accelerated rate before the diode case temperature. In addition to finding evidence for the root cause of the failures during prototype PPU testing, data from this investigation show the superior performance of Diode Z parts and support its selection for use in the NEXT-C flight PPUs.

The failure investigation team has plans to conduct testing of the brassboard beam module in vacuum, to eliminate the effects of convection cooling on the diodes and better control the thermal environment, to quantify the margin of the NEXT-C beam module design in terms of beam module output current and operating baseplate temperature. This information is critical for future applications of the NEXT-C system that will require operation at full power conditions.

References

[1] Fisher, Jack., et al., “NEXT-C Flight Ion System Status", AIAA-2020-3604, AIAA Propulsion and Energy Forum, August 24-26, 2020.

[2] Patterson, M. and Benson, S., “NEXT Ion Propulsion System Development Status and Performance,” AIAA 2007- 5199, 43rd Joint Propulsion Conference, Cincinnati, OH July 2007.

[3] Patterson, M. J., Foster, J., Haag, T., Piñero, L., Rawlin, V., and Roman, R., "Next-Generation 5/10 kW Ion Propulsion System", IEPC Paper 01-089, 27th International Electric Propulsion Conference, Los Angeles, October 15-19, 2001.

[4] Piñero, L. R. and Benson, S. W., "NEXT Engineering Model PPU Development, Progress and Plans", AIAA-2011-5659, 47th AIAA Joint Propulsion Conference, San Diego, California, July 31 - August 3, 2011.

[5] Piñero, L. R., Hopson, M., Todd, P. C., and Wong, B., “Performance of the NEXT Engineering Model Power Processing Unit”, AIAA-2007-5214, 43rd Joint Propulsion Conference, Cincinnati, OH, July 8-11, 2007.

[6] Todd, P., Martinelli, R., Wiseman, S., and Piñero, L., “Status of the NEXT 7 kW Power Processing Unit”, AIAA-2005-3868, 41st Joint Propulsion Conference, Tucson, Arizona, July 10-13, 2005.

[7] Phelps T., Wiseman S., Komm, D., Bond, T., and Piñero, L., “Development of the NEXT Power Processing Unit” AIAA Paper 2003-4867, 39th Joint Propulsion Conference, Indianapolis, Indiana, July 7-10 , 2002.

[8] Piñero, L. R., Bond, T., Okada, D., Phelps, K., Pyter, J., and Wiseman, S., "Design of a Modular 5-kW Power Processing Unit for the Next-Generation 40-cm Ion Engine", IEPC Paper 01-329, 27th International Electric Propulsion Conference, Los Angeles, October 15-19, 2001.

[9] Bontempo, J. J., Brigeman, A. N., Fain, H. B., Gonzalez, M. C., Piñero, L. R., Aulisio, M. V., Birchenough, A. G., Fisher, J. R., and Ferraiuolo, B., "The NEXT-C Power Processing Unit: Lessons Learned from the Design, Build, and Test of the NEXT-C PPU for APL's DART Mission", AIAA-2020-3641, AIAA Propulsion and Energy Forum, August 24-26, 2020.

[10] Aulisio, M. V., Piñero, L. R., White, B. L., Hickman, T. A., Bontempo, J. J., Hertel, T. A., and Birchenough, A. G., "Status of the Development of Flight Power Processing Units for the NASA’s Evolutionary Xenon Thruster – Commercial (NEXT-C) Project ", AIAA-2016, 4519, 52nd AIAA Joint Propulsion Conference, Salt Lake City, Utah, July 25-27, 2016.